In summary, the drag coefficient of slender bodies of revolution in the hypersonic near-continuum and transitional regimes has a minimum for $\theta = O(1)$. Analytic flow models that apply for $\bar{v} > 0.10$ (forward of the strong-interaction regime) are clearly needed. A first-order estimate of an average flight condition for skip trajectories and very low orbits of powered satellites is presented that depends on the drag-coefficient curve, but not on the trajectory or atmospheric details.

References

[1] Mirels, H. and Ellinwood, J. W., "Viscous Interaction Theory for Slender Axisymmetric Bodies in Hypersonic Flow," *AIAA Journal*, Vol. 6, No. 11, Nov. 1968, pp. 2061–2070.

[2] Kussoy, M. I. and Horstman, C. C., "Cone Drag in Rarefied Hypersonic Flow," AIAA Paper 69-140, New York, 1969.

[3] McCroskey, W. J., Bogdonoff, S. M., and Genchi, A. R., "Leading Edge Flow Studies of Sharp Bodies in Rarefied Hypersonic Flow," *5th International Symposium on Rarefied Gas Dynamics*, Vol. II, Academic Press, New York, 1967, pp. 1047–1066.

Nonlinear Ballistic Wind Compensation of Unguided Ballistic Rocket Systems

GERALD G. WILSON*
Sandia Laboratories, Albuquerque, N. Mex.

Nomenclature

D	=	deflection normal to corrected azimuth, or constant related to range, m
K	=	constants related to nonlinear coefficients, sec, or empirical equations, m/sec
l	=	exponent related to nominal range
m,n	=	exponents related to down- and cross-range wind effects, respectively
R	=	range, m
u,v	=	east-west (or parallel) and north-south (or normal) ballistic wind velocity components, respectively, m/sec
V	=	total ballistic wind velocity, m/sec
X,Y,Z	=	axes, positive northward, eastward, and downward, respectively, m
θ	=	launcher elevation angle measured from horizontal, deg
λ	=	directions from which the ballistic wind blows, deg
η	=	launcher azimuth angle, deg

Superscript

$'$	=	combined constants

Subscripts

0	=	nominal no-wind or condition required for vertical launcher setting
N	=	nominal or normal component
P	=	parallel component
K	=	constant associated with range
1,2	=	constant associated with down- and cross-range wind effect, respectively

Introduction

IMPACT-POINT prediction for unguided ballistic rocket systems, in the presence of surface winds, must involve solution of the six-degree-of-freedom equations of motion.[1,2]

Received August 13, 1969; revision received September 29, 1969. This work was supported by the U. S. Atomic Energy Commission.

* Staff Member in the Aerothermodynamic Projects Department. Associate AIAA.

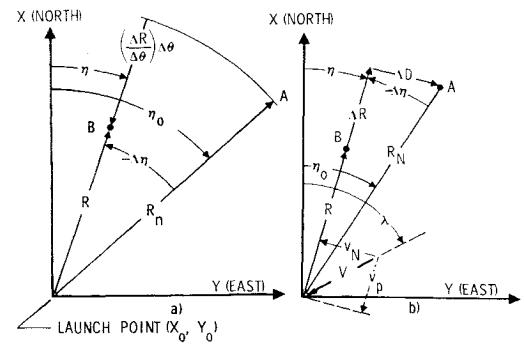

Fig. 1 Schematics of rocket trajectories without and with a ballistic wind.

The effects of system tolerances on trajectory dispersion can be reduced by aerodynamically designing the system to have a large static margin at rocket ignition. However, a large static margin at launch causes the wind effects to become a major contributor to dispersion. Vehicle dispersion can be further reduced by using both an induced roll rate and a launcher with rail guidance[3]; however, a maximum of ~5m of rail guidance is effective with most unguided systems. Numerous methods for determining launcher settings have been proposed (e.g., Refs. 4–8). These methods involve using point mass trajectories for wind effects, assuming that down-range and cross-range wind effects are identical for all elevations angles of interest, "near-vertical" launches, extensive and time-consuming graphical techniques, and other undesirable features. This Note presents a linear wind compensation method used very successfully by Sandia Laboratories since 1959.† The linear technique is extended to account for the nonlinear changes in down- and cross-range wind effects with elevation angle, and is used to derive a form of the empirical nonlinear equations established by Walker.[5]

Equations with Linear Wind Effects Coefficients

It is assumed that the altitude-wind profile obtained near the time of launch is effectively reduced by a wind-weighting system to a ballistic wind of magnitude V blowing at an angle λ. All angles are measured by the right-hand rule from the X axis, with the exception of the elevation angle θ, which is measured positive-upward from the X, Y plane. Instead of using the X, Y, Z coordinates, we use θ, range R, and deflection from the corrected azimuth D to specify the vehicle location. Figure 1a shows the projection of ballistic rocket trajectories onto the X, Y plane. When no ballistic wind is present, the R for a new launcher setting (η,θ) may be obtained by

$$R = R_N + (\Delta R/\Delta\theta)\Delta\theta = R_N + (\Delta R/\Delta\theta)(\theta - \theta_0) \quad (1)$$

where R_N and θ_0 are the nominal values, and $\Delta R/\Delta\theta$ is negative for a positive $\Delta\theta$ at large θ's. [For θ's below the θ for maximum range $(\Delta R/\Delta\theta)$ changes sign.]

When a ballistic wind acts on the system (Fig. 1b), the launcher, to compensate, must be moved through $\Delta\eta$ and $\Delta\theta$; the correct changes will cause the vehicle to pass through the nominal aiming point A. Expressions for ΔD and ΔR are obtained from Fig. 1b, and the expression for ΔR is combined with Eq. (1) to give

$$\Delta D = -R_N s\Delta\eta \quad (2)$$

$$\Delta R = R_N(c\Delta\eta - 1) - (\Delta R/\Delta\theta)\Delta\theta \quad (3)$$

† The original equations using linear (or constant) coefficients were developed by H. A. Wente, Staff Member, Aerothermodynamics Projects Department, Sandia Laboratories, Albuquerque, N. Mex.

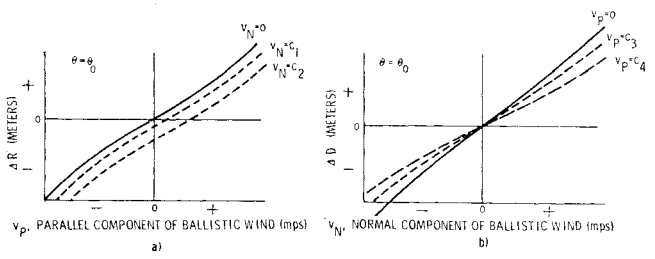

Fig. 2 Variations of range and deflection with ballistic wind components.

where c ≡ cosine and s ≡ sine. To determine ΔR and ΔD, it is necessary to consider these quantities as functions of $\Delta\theta$ and the ballistic wind components, V_N and V_P (normal and parallel to the corrected azimuth, respectively). Figure 2 shows range and deflection variations with V_N and V_P for a given θ; these curves are typical for a ballistic, fin-stabilized rocket. For a vehicle launched at high θ, having large launch accelerations and comparatively linear aerodynamics, such curves tend to coalesce and approach the same slope about the origin for small changes in θ. Under these conditions, ΔR and ΔD can be assumed to be independent of V_N and V_P, respectively. The expressions for ΔR and ΔD can then be written

$$\Delta R = (\partial R/\partial V_P)V_P = (\partial R/\partial V)\ V\mathrm{c}\xi \tag{4}$$

$$\Delta D = (\partial D/\partial V_N)V_N = (\partial D/\partial V)V\mathrm{s}\xi \tag{5}$$

where $\xi = \lambda - \eta_0 - \Delta\eta$. The subscript notation in the partial derivatives has been dropped for convenience, and the expressions for V_N and V_P are obtained from Fig. 1b. Equations (3) and (4), and (2) and (5) are combined to yield

$$(\partial R/\partial V)V\mathrm{c}\xi = R_N(\mathrm{c}\Delta\eta - 1) - (\partial R/\partial\theta)\Delta\theta \tag{6}$$

$$(\partial D/\partial V)V\mathrm{s}\xi = -R_N\mathrm{s}\Delta\eta \tag{7}$$

Equations (6) and (7) contain the four unknowns λ, $\Delta\eta$ (also in ξ), $\Delta\theta$, and V. It is possible to assume values of two of the unknowns and solve for the remaining unknowns. For launcher set chart construction, values of $\Delta\theta$ and $\Delta\eta$ are assumed, and the equations are solved for λ and V. Polar coordinates are used to locate λ and V along the angular and radial coordinates, respectively. Lines of constant $\Delta\eta$ and $\Delta\theta$ are constructed graphically to facilitate locating the correct launcher setting, as shown in Fig. 3. The equations can be programmed on relatively small digital computers to aid in determining launcher settings at the launch site. The magnitude of the ballistic wind and its direction are known, and the equations are solved for $\Delta\theta$ and $\Delta\eta$.

The impact point of any portion of the rocket system may be determined from Fig. 1b by summing the components in the X and Y directions to give

$$X = X_0 + (R + \Delta R)\mathrm{c}\eta - \Delta D\mathrm{s}\eta \tag{8}$$

$$Y = Y_0 + (R + \Delta R)\mathrm{s}\eta + \Delta D\mathrm{c}\eta \tag{9}$$

Table 1 Single-stage Sandhawk rocket system impact range

θ, deg	R_{theo},[a] m	R, Eq. (12), m	% error
70	230,289	231,668	0.60
74	200,937	201,778	0.42
78	161,090	161,269	0.11
80	137,779	137,779	0
84	85,835	85,733	0.12
86	57,898	57,746	0.26
88	29,152	29,432	0.96

[a] R_{theo} impact range determined by five-degree-of-freedom trajectory simulation.

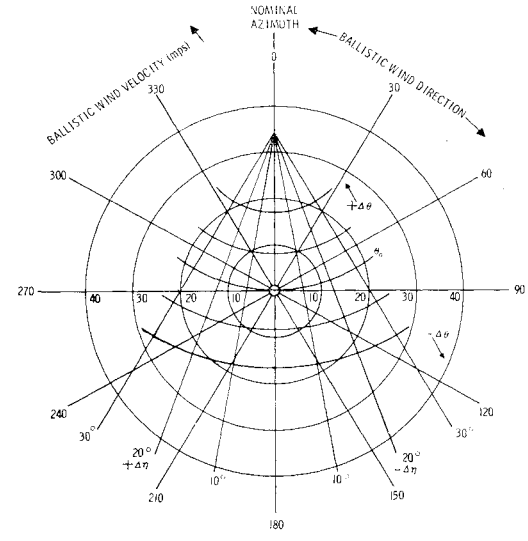

Fig. 3 Launcher set chart based on linear coefficients.

Substitution for the expressions in Eq. (8) gives

$$X = X_0 + [(\partial R/\partial\theta)\Delta\theta + R_N]\mathrm{c}\eta + (\partial R/\partial V)V\mathrm{c}\xi\mathrm{s}\eta - (\partial D/\partial V)V\mathrm{s}\xi\mathrm{s}\eta \tag{10}$$

and a similar equation is obtained for Y. The appropriate values of the constants and coefficients are provided for each stage or component part to yield its respective impact location.

Equations with Nonlinear Wind Effects Coefficients

The equations used to determine Fig. 3 do not necessarily permit a singular point for $\theta = 90°$ as would be expected for a vehicle having threefold[9] or greater symmetry. Schaechter[10] has shown that $R(\theta)$ for a sounding rocket can be closely approximated by

$$R = D_K\mathrm{s}^l\theta\mathrm{c}\theta \text{ or } R_N = D_K\mathrm{s}^l\theta_0\mathrm{c}\theta_0 \tag{11}$$

where D_K, a constant, and l on the sine term are characteristic of a given rocket system. Equation (11) was applied to the single-stage Sandhawk,[11] (Table 1) and agreement was reasonably good.

The $\partial R/\partial V$ and $\partial D/\partial V$ were assumed constant for the determination of Fig. 3. They were determined by five-degree-of-freedom trajectory simulation[2] and are functions of θ, as shown for Sandhawk in Fig. 4, and can be adequately represented by

$$\partial R/\partial V = -K_1(m\mathrm{s}^{m-1}\theta\mathrm{c}\theta - \mathrm{s}^{m+1}\theta),\ \partial D/\partial V = K_2\mathrm{s}^n\theta \tag{12}$$

where m, n, K_1, and K_2 are rocket-system-dependent. When $\theta = 90°$, the $\partial R/\partial V = \partial D/\partial V$, so that $K_1 = K_2$. Equations (2) and (3) are formulated to read

$$\Delta D = -R_N\mathrm{s}\Delta\eta,\ \Delta R = R_N\mathrm{c}\Delta\eta - R \tag{13}$$

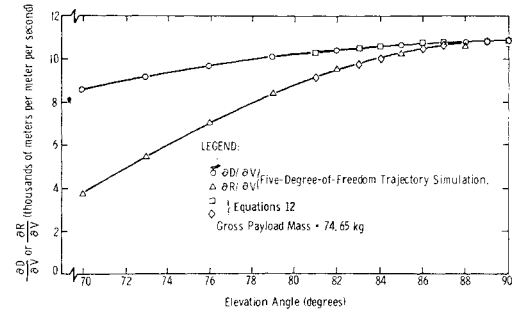

Fig. 4 Single-stage Sandhawk wind effects partials.

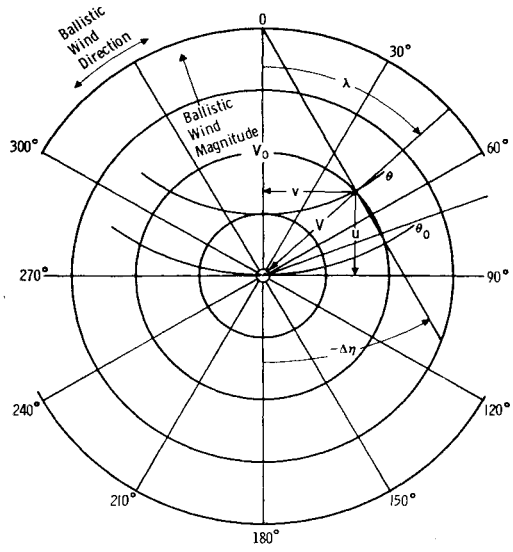

Fig. 5 Generalized launcher set chart.

Equations (11, 4, and 5), combined with (12), are used in Eqs. (13) to give

$$-K_1(ms^{m-1}\theta c\theta - s^{m+1}\theta)V_P = D_K s^l\theta_0 c\theta_0 c\Delta\eta - D_K s^l\theta c\theta \quad (14)$$

$$K_1(s^n\theta)V_N = -D_K s^l\theta_0 c\theta_0 s\Delta\eta \quad (15)$$

These equations were solved and compared with the results of Eqs. (6) and (7). The amount of improvement in the launcher settings by using Eqs. (14) and (15) was insignificant for small changes in θ. However, a single-valued point at $\theta = 90°$ was obtained. Equation (14), evaluated at $\theta = 90°$ and $\Delta\eta = 0$, gives

$$K_1V_P = R_N \text{ or } V_0 = R_N/K_1 \quad (16)$$

where V_0 is that magnitude of ballistic head wind that would require a vertical launcher setting for impact at the desired nominal R_N for the nominal θ_0.

Walker's Empirical Nonlinear Equations

Walker[5] derived empirical equations by curve-fitting ballistic firing table data plotted on rectangular ballistic wind coordinates. By using polar coordinates to represent the ballistic winds, Walker's method can be generalized for greater utility. From Fig. 5,

$$\tan\Delta\eta = -v/(V_0 - u) \quad (17)$$

and

$$\tan(90 - \theta) = [(V_0 - u)^2 + v^2]^{1/2}/K \quad (18)$$

where u and v are the ballistic wind velocity components parallel (positive for head wind), and normal (positive from right side) to the nominal launch azimuth, respectively; K is an empirical constant related to launcher-tilt effect. The constants in Eqs. (17) and (18) are independent of η while the constants in Walker's equations are η-dependent.

Derivation of Walker's Equations from the Equations with Linear Wind Effects Coefficients

The linear scheme must utilize V_N and V_P, which, from Fig. 1b, become

$$V_N = vc\Delta\eta - us\Delta\eta,\ V_P = uc\Delta\eta + vs\Delta\eta \quad (19)$$

The assumption is made that the equations will be evaluated for θ's near 90°, so that the values of the wind effects partials can be replaced by the constant K_1, determined from Eqs. (12). Equation (13) for ΔD combined with (5) and (19) for V_N gives

$$K_1(vc\Delta\eta - us\Delta\eta) = +R_N s\Delta\eta \quad (20)$$

Dividing Eq. (20) by $c\Delta\eta$ and solving $\tan(\Delta\eta)$, and using (16) gives Eq. (17). Equation (13) for ΔR, combined with (4) and (19) for V_P gives

$$K_1(uc\Delta\eta + vs\Delta\eta) = R_N c\Delta\eta - R \quad (21)$$

R represented by Eq. (11) can be written

$$R = D_K s^l\theta c\theta = D_K s^{l+1}\theta \cot\theta = -K' \tan(90° - \theta) \quad (22)$$

and utilized in (21) to yield

$$-K'\tan(90° - \theta) = K_1(uc\Delta\eta + vs\Delta\eta) - R_N c\Delta\eta \quad (23)$$

The expressions for $c\Delta\eta$ and $s\Delta\eta$ obtained from Fig. 5 are used in (23) along with $V_0 = R_N/K_1$, which gives Eq. (18), and because of the assumptions used in its formulation, should be valid for only "near-vertical" firings. However, for nonlinear use, the expressions for V_0 and K cannot be formulated from linear wind effect coefficients. Equations (17) and (18) were evaluated for θ's as low as 75° for the ballistic firing tables[5] and for θ's as low as 80° for the nonlinear wind analysis,[6] and excellent agreement was found in both cases.

Conclusions

The nonlinear wind effect coefficient equations, for the assumption of "near-vertical" launches, reduce to a form of the empirical equations established by Walker. The nonlinear equations are not restricted to near-vertical firings, and are independent of assumptions regarding down- and cross-range wind effectiveness. The nonlinear equations are applicable over a wide range of elevation angles, and the accuracy of the equations is comparable to very sophisticated and costly firing tables and to the nonlinear analyses, while omitting the necessary time-consuming iterations for accurate solution.

The constants in the nonlinear equations require elevation by at least five-degree-of-freedom trajectory, and a maximum of two simulations are required to determine the constants for a given nominal elevation angle.

References

[1] Etkin, B., "General Equations of Unsteady Motion," *Dynamics of Flight*, Wiley, New York, 1959, pp. 94–144.

[2] "Six-Degree-of-Freedom Flight-Path Study Generalized Computer Program," FDL-TDR-64-1, Oct. 1964, Air Force Flight Dynamics Lab., Wright-Patterson Air Force Base, Ohio.

[3] Denkmann, W. J., "Variations of the Trajectory of an Unguided Rocket Caused by Statistical Variations in Parameters," SUI-ORD-1232-R-9, Phase V, Pt. I, Nov. 1963, State Univ. of Iowa, Iowa City, Iowa.

[4] Hennigh, K. E., "Field Wind Weighting and Impact Prediction for Unguided Rockets," TN-D-2142, March 1964, NASA.

[5] Walker, R. L., "Improved Method of Obtaining Launcher Settings," Space Data Corp., Phoenix, Ariz., presented at Unguided Ballistics Meteorology Conference, Texas Western Univ., El Paso, Texas, Sept. 1, 1966.

[6] Wilson, G. G., "A Technique for Predicting Nonlinear Wind Compensation of Ballistic Rocket Systems," Sandia Labs., Albuquerque, N. Mex., presented at Unguided Ballistic Meteorology Conference, New Mexico State Univ., Las Cruces, N. Mex., Oct. 31–Nov. 2, 1967.

[7] James, R. L., Jr. and Harris, R. J., "Calculation of Wind Compensation of Unguided Rockets," TN-D-645, Oct. 1960, NASA.

[8] Henning, A. B., Lundstrom, R. R., and Keating, J. C., "A Wind-Compensation Method and Results of Its Application to Flight Tests of Twelve Trailblazer Rocket Vehicles," TN-D-2053, Sept. 1963, NASA.

[9] Maple, C. G. and Synge, J. L., "Aerodynamic Symmetry of Projectiles," *Quarterly of Applied Mathematics*, Vol. VI, No. 4, Jan. 1949, pp. 345–366.

[10] Schaechter, W., "Sounding Rocket Performance Approximations," Thiokol Chemical Corp., Ogden, Utah, presented at Unguided Rocket Ballistics Meteorology Conference, New Mexico State Univ., Las Cruces, N. Mex., Oct. 31–Nov. 2, 1967.
[11] Wilson, G. G., "Aeroballistic, Performance, Wind Effects and Payload Impact Dispersion and Flight Test Data for the Single-Stage Sandhawk Rocket System," SC-DR-291, July 1969, Sandia Labs., Albuquerque, N. Mex.

Numerical Analysis of Low-g Propellant Flow Problems

R. A. Madsen,* C. R. Easton,* and G. W. Burge†
McDonnell Douglas Astronautics Company, Western Division, Santa Monica, Calif.
AND
I. Catton‡
University of California, Los Angeles, Calif.

Introduction

The Marker- and Cell (MAC) numerical technique is capable of analyzing many of the low-g fluid flow and heating problems encountered with liquid propellant storage and supply systems. It can be used to calculate transient two-dimensional viscous flow and heating of fluid in a partially filled tank (which may contain baffles or an unusual initial liquid-vapor interface), for arbitrary prescribed initial and boundary conditions. Behavior of the liquid-vapor interface is calculated and interface breakup is permitted. An animated motion picture depicting the motion of the fluid, which is furnished as a portion of the computer output, is invaluable for rapidly assessing over-all features of calculated results. A detailed description of the MAC technique is presented in Ref. 1. Therefore only a brief description is given here.

The Navier Stokes and thermal-energy equations are cast in finite-difference form and solved explicitly as an initial value problem. A Poisson equation, derived from continuity, is solved for pressure by the Gauss-Seidel iterative method. For laminar flow with constant properties, the only approximation fundamental to the technique is that attributed to the finite-difference representation of the equations and the boundary conditions. Further approximations, such as linearizing equations or neglecting viscous effects are not necessary.

Typical meshes of computational cells are shown in Figs. 1–3. Velocities ($u_{i,j}$ and $u_{i+1,j}$, and $v_{i,j}$ and $v_{i,j+1}$) are defined on the sides of each cell. Pressure, temperature, and mass dilatation are defined at the center of each cell. At a rigid wall, either a free-slip velocity boundary condition (vanishing normal velocity component), or a no-slip velocity boundary condition (vanishing normal and tangential velocity components) can be applied. The free-slip condition, used herein, is appropriate when the thickness of the hydrodynamic boundary layer is much less than the width of a calculational cell. Boundary conditions at the liquid-vapor interface are selected to make the tangential shear stress vanish, to make the normal stress equal to the applied pressure, and to satisfy continuity in each surface cell. At an outlet cell, the outlet velocity history is prescribed and the required pressure gradient is determined from the momentum equation. Thermal boundary conditions are not of interest herein, because thermal effects were not considered in the examples presented.

Marker particles are set up as the numerical equivalent of neutrally buoyant particles used in laboratory flow-visualization experiments. They establish the location of the free surface and provide a visual display of fluid motion in computer-generated plots (Figs. 1–3). Marker particles are moved according to the local velocity at the end of each time step. The frames shown in Figs. 1–3 were printed directly from the microfilm output of a Stromberg Datagraphics SD-4060 microfilm recorder. After printing, outstanding features were overlayed on the prints.

Propellant Disturbances During Docking

A study was made of the propellant disturbances that could be expected in the LH_2 tank of the Saturn S-IVB stage

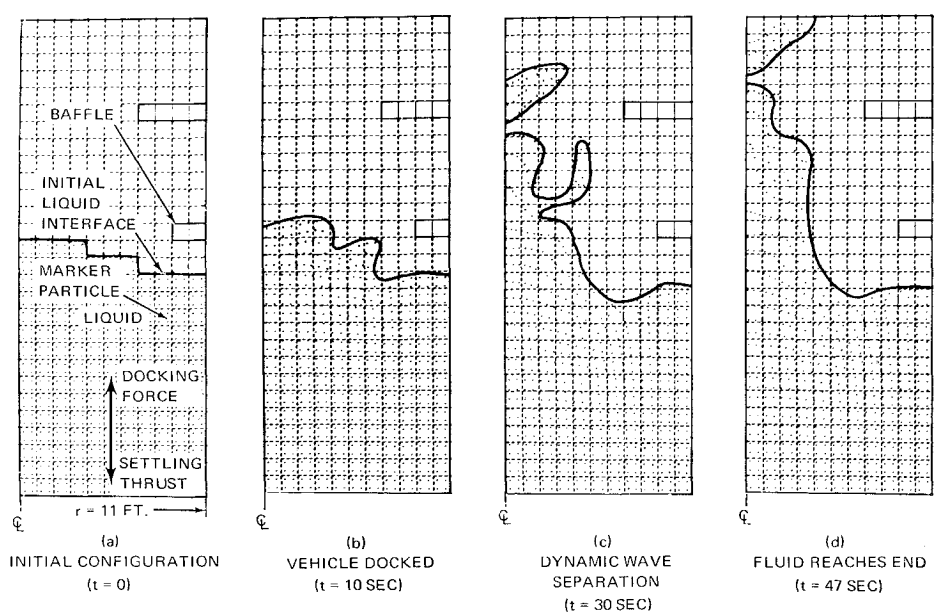

Fig. 1 Symmetric propellant unsettling.

Presented as Paper 69-567 at the AIAA 5th Propulsion Joint Specialist Conference, U.S. Air Force Academy, Colo., June 9–13, 1969; submitted July 11, 1969; revision received September 15, 1969. Portions of this work were sponsored by the NASA George C. Marshall Space Flight Center under Contract NAS 7-101.

* Senior Engineer Scientist, Advance Propulsion Department.
† Branch Chief, Liquid Propulsion Subsystems, Advance Propulsion Department. Member AIAA.
‡ Assistant Professor of Engineering. Member AIAA.